
This is an electronic reprint of the original article.
This reprint may differ from the original in pagination and typographic detail.

Makkonen, I.; Snicker, A.; Puska, M.J.; Mäki, J.-M.; Tuomisto, F.

Positrons as interface-sensitive probes of polar semiconductor heterostructures

Published in:
Physical Review B

DOI:
[10.1103/PhysRevB.82.041307](https://doi.org/10.1103/PhysRevB.82.041307)

Published: 01/07/2010

Document Version
Publisher's PDF, also known as Version of record

Please cite the original version:
Makkonen, I., Snicker, A., Puska, M. J., Mäki, J.-M., & Tuomisto, F. (2010). Positrons as interface-sensitive probes of polar semiconductor heterostructures. *Physical Review B*, 82(4), 1-4. [041307].
<https://doi.org/10.1103/PhysRevB.82.041307>

This material is protected by copyright and other intellectual property rights, and duplication or sale of all or part of any of the repository collections is not permitted, except that material may be duplicated by you for your research use or educational purposes in electronic or print form. You must obtain permission for any other use. Electronic or print copies may not be offered, whether for sale or otherwise to anyone who is not an authorised user.

Positrons as interface-sensitive probes of polar semiconductor heterostructures

I. Makkonen,¹ A. Snicker,² M. J. Puska,² J.-M. Mäki,² and F. Tuomisto²

¹*Helsinki Institute of Physics and Department of Applied Physics, Aalto University, P.O. Box 14100, FI-00076 AALTO, Espoo, Finland*

²*Department of Applied Physics, Aalto University, P.O. Box 11100, FI-00076 AALTO, Espoo, Finland*

(Received 30 March 2010; revised manuscript received 9 July 2010; published 23 July 2010)

Group-III nitrides in their wurtzite crystal structure are characterized by large spontaneous polarization and significant piezoelectric contributions in heterostructures formed of these materials. Polarization discontinuities in polar heterostructures grown along the (0001) direction result in huge built-in electric fields on the order of megavolt per centimeter. We choose the III-nitride heterostructures as archetypal representatives of polar heterostructures formed of semiconducting or insulating materials and study the behavior of positrons in these structures using first-principles electronic-structure theory supported by positron annihilation experiments for bulk systems. The strong electric fields drive positrons close to interfaces, which is clearly seen in the predicted momentum distributions of annihilating electron-positron pairs as changes relative to the constituent bulk materials. Implications of the effect to positron defect studies of polar heterostructures are addressed.

DOI: [10.1103/PhysRevB.82.041307](https://doi.org/10.1103/PhysRevB.82.041307)

PACS number(s): 78.70.Bj, 73.40.Kp, 77.84.Bw

Semiconductor heterostructures are the core elements of electronic and especially optoelectronic semiconductor devices, such as light-emitting diodes and laser diodes (LDs). The materials family of choice for blue and ultraviolet optoelectronics, with the potential for covering the whole spectral range down to infrared, is that of the group-III nitrides AlN, GaN, and InN. Ideally it is the design of the structure that defines the properties of the device at hand but in practice the structural quality of the semiconductor materials themselves and the heterointerfaces between them often limit significantly the output.¹ This is the case especially in device structures fabricated out of III-nitrides due to the large lattice mismatch of the constituent materials. Hence, even if it was possible to grow thin layers of III-nitrides, or more specifically their ternary alloys such as In_{0.13}Ga_{0.87}N, without defects in the bulk of the layer, the interfaces between, e.g., the quantum wells and barriers in a LD are likely to have complicated structures leading to generation of extended defects detrimental to the functioning of the device.

In addition to extended defects such as stacking faults and dislocations, point defects have a significant impact on the electrical and optical properties of the nitride semiconductor materials.² Positron annihilation spectroscopy is a method particularly well suited for studying vacancy defects in semiconductors (for a review see Ref. 3). During the past decade it has been applied in numerous studies where the identities, concentrations, and characteristics of both in-grown and process-induced vacancy defects in nitride semiconductors have been determined (see, e.g., Refs. 4–6, and the references therein). Recently, there have been also attempts to understand the data obtained with positron annihilation spectroscopy in InGaN alloys assuming the presence of low-dimensional nitride structures such as spatial fluctuations in In content.⁷

In this Rapid Communication we explore the potential of positron annihilation spectroscopy in studying semiconductor, especially III-nitride, heterostructures. In the III-nitrides with the wurtzite structure the lack of inversion symmetry causes spontaneous polarization in the (0001) direction. The heterostructures are usually grown along this direction and therefore they show, in addition to the band-gap modulation

essential for functioning of electronic devices, electric fields created by the polarization discontinuities at the interfaces.^{8–10} We will show that, in addition to being able to probe defects inside the bulk materials in these structures, positrons in polar heterostructures are sensitive to the interface regions as well. The electric fields in these structures cause positrons to favor regions near interfaces although vacancy defects may trap positrons regardless of their location. To study the problematics we use state-of-the-art *ab initio* computational methods benchmarked by positron experiments for III-nitride materials. Our calculations show that momentum distributions of annihilating electron-positron pairs probed in the measurements of the Doppler broadening of the annihilation radiation are especially sensitive in characterizing the annihilation environment in these structures. We find in our calculations that positron lifetime, as an integrated quantity, is a less sensitive indicator, and therefore, lifetime data is not presented here.

We model the nitride materials and heterostructures using density-functional calculations and periodic models. Electronic and ionic structures are calculated self-consistently using the local-density approximation and the projector augmented-wave method¹¹ implemented in the plane-wave code VASP.¹² For a detailed description of the methodology of our positron calculations see Ref. 13. Most importantly, the positron potential constructed is effectively an all-electron potential, and the all-electron wave functions are reconstructed. Having an accurate potential is important when modeling positron energy landscapes in heterostructures.

The Doppler broadening of the 511 keV annihilation line is due to the electron momenta at the site of the annihilation. Since the atom-specific core electron contributions dominate at high momenta, the Doppler signal at this region gives chemical information on the annihilation site. In particular, in III-nitrides the outermost cation *d* electrons have characteristic “fingerprints” that are displayed clearly in measurements made for well-characterized bulk materials samples and can be used to analyze nitride heterostructure results.

We start by considering first the bulk nitrides AlN, GaN, and InN in order to assess our theoretical predictions. Figure

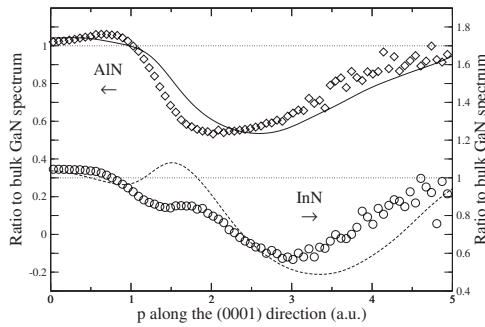


FIG. 1. Comparison of experimental and computational Doppler spectra of AlN and InN normalized to that of GaN. The markers and curves denote the measured and calculated results, respectively.

1 shows the comparison between computational and experimental Doppler spectra of AlN and InN normalized to that of GaN. The experimental positron annihilation studies are carried out using a variable energy ($E=0-40$ keV) positron beam.³ The implantation energy of 20 keV we use is enough to guarantee that the positrons annihilate in the bulk of the sample. In order to reduce the peak-to-background ratio we measure the annihilation photons in coincidence with two high-purity Ge detectors.^{5,6} To facilitate the comparison with experimental spectra the theoretical spectra are convoluted with the experimental momentum resolution of 0.5 a.u. Our computations are able to reproduce the qualitative features of the experimental spectra. The high-momentum features of the ratio spectra are reproduced well qualitatively, which is important for the chemical analysis. The peak (or shoulder) at around 1.5–2 a.u. in the InN ratio spectrum exists also in the computational data although its intensity is overestimated. Below this momentum regime the signal is dominated by low-momentum valence electrons and above it by high-momentum core electrons. Accurate quantitative description of the spectra at this transition region is difficult. The comparison in Fig. 1 justifies the use of our modeling scheme in predicting Doppler spectra for the more complex nitride heterostructures.

The nitride heterostructures modeled in this work are superlattices formed of AlN and GaN or of InN and GaN having equal numbers of atomic layers. We study both nonpolar a -plane and polar c -plane wurtzite heterostructures corresponding to growth along the $(11\bar{2}0)$ and (0001) directions, respectively. The layer thicknesses are at least 2 nm, i.e., same order as in realistic optoelectronic components. In addition to their strong spontaneous polarization the wurtzite III-nitrides have large piezoelectric constants,⁹ and therefore, the macroscopic polarization at the nitride heterostructures depends strongly on strain conditions. Especially in our models for heterostructures consisting of GaN and InN the piezoelectric contributions are large due to the large lattice-constant mismatch between the constituent materials. For each nitride pair (e.g., AlN and GaN) and growth direction we build two models corresponding to different strain conditions. For example, we constrain AlN to the in-plane lattice constant of GaN in the model denoted by GaN/AlN and vice versa in AlN/GaN. Thus, in the notation the first nitride determines the in-plane lattice constant. The axial lattice con-

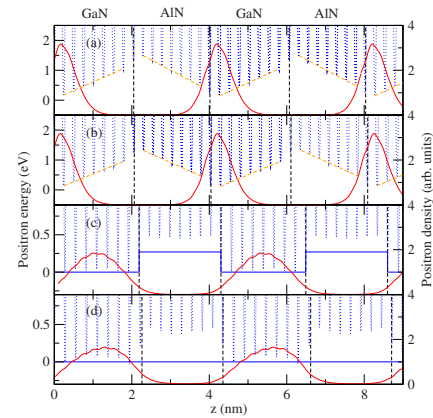


FIG. 2. (Color online) Macroscopic averages of the positron density (red solid curves) in (a) GaN/AlN(0001), (b) AlN/GaN(0001), (c) GaN/AlN($11\bar{2}0$), and (d) AlN/GaN($11\bar{2}0$) heterostructures. The positron potentials averaged over the planes perpendicular to the interface normal are also shown (dotted blue curves). For the polar structures in (a) and (b) the straight envelope lines through the potential minima are shown whereas for the nonpolar structures in [(c) and (d)] the energy difference between the straight horizontal lines reflects the positron energy offset between the adjacent layers.

stants and the internal parameters of the strained layers are determined by energy minimization. Then, after attaching the two nitride layers together, the ionic positions are fully relaxed. Below we analyze the effects of the choice of materials, growth direction, polar vs nonpolar, and strain on the behavior of the positron state and on the Doppler spectra. We will also discuss the effects of possible vacancy defects.

Figures 2 and 3 show the positron densities in the different polar and nonpolar heterostructures with different strain conditions. The atomic-scale variations are smoothed out as in Ref. 14 by first averaging over planes perpendicular to the interface normal and finally convoluting the resulting one-dimensional data. In the case of the nonpolar heterostructures the density is typically confined rather symmetrically in the GaN layer with the exception of the GaN/InN($11\bar{2}0$) structure in Fig. 3(c). In this case the in-plane lattice parameters

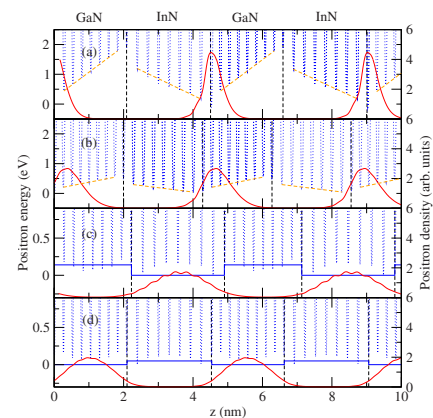


FIG. 3. (Color online) Same as Fig. 2 for polar (a) GaN/InN(0001) and (b) InN/GaN(0001), as well as for nonpolar (c) GaN/InN($11\bar{2}0$) and (d) InN/GaN($11\bar{2}0$) heterostructures.

are those of GaN, i.e., the InN layer is under compressive strain. However, it relieves stress by expanding in the growth direction, which leads to lowered atomic density and positron's preference to InN. In the polar structures the polarization discontinuities at the interfaces induce net polarization charges (interface monopoles) at the interfaces.⁸ These charges, in turn, induce macroscopic electric fields across the nitride layers driving the positron density toward one of the two interfaces in the heterostructure, the one where holes are driven too. Thus, in the absence of open volume defects capable of trapping positrons, positrons probe the interface region of the heterostructure.

The formation of the macroscopic electric fields can be seen in electrostatic potentials averaged using the scheme described for the positron density above.^{8,14} However, the averaged potential does not reflect well the behavior of the positron density because positrons prefer strongly the interstitial regions. Therefore, we plot in Figs. 2 and 3 the positron potential averaged over planes perpendicular to the interface normal but skip the above-mentioned convolution along the growth direction. In the case of polar structures the straight envelope lines drawn through the potential minima illustrate the effect of the macroscopic electric fields and indicate clearly the low-potential regions near interfaces preferred by the positron. The variation in the macroscopic potential across a layer is on the order of 1 eV. There are also rather abrupt potential jumps across the interfaces caused by the interface dipole charges.^{8,14} In polar wurtzite heterostructures the two interfaces lack inversion symmetry and thus their dipoles and potential jumps may differ in magnitude.

In the case of nonpolar heterostructure models the minima of the averaged positron potential display a rather symmetric behavior across the layers. These minima, however, cannot exclusively predict the preference of the positron to a certain layer in a given structure. For these structures we can determine how much energy it costs to move a positron confined in the more attractive layer to the opposite one. We call this energy positron energy offset and estimate it as follows. We shift the positron potential rigidly in the nitride layer in which the positron density is confined in the equilibrium case, for instance, in the GaN layer in the case of the nonpolar heterostructures in Fig. 2. The shift that is just enough to move the positron density to the opposite nitride layer corresponds to the positron energy offset between these two layers in the specific heterostructure. For sufficiently wide layers the result is specific to the interface between the two layers in the structure in question.

We obtain the positron energy offsets of +0.27 eV, 0.00 eV, -0.14 eV, and +0.05 eV for GaN/AlN(11 $\bar{2}$ 0), AlN/GaN(11 $\bar{2}$ 0), GaN/InN(11 $\bar{2}$ 0), and InN/GaN(11 $\bar{2}$ 0), respectively, the positive sign meaning that the GaN layer is more attractive. The above energies are rather small, so small that they are considerably affected by the strain conditions. This is true even for the GaN- and AlN-containing heterostructures, for which the lattice-constant mismatch is small. For the nonpolar heterostructures in Figs. 2 and 3 the energy differences between the horizontal straight lines reflect the positron energy offsets correlating with the positron density distributions.

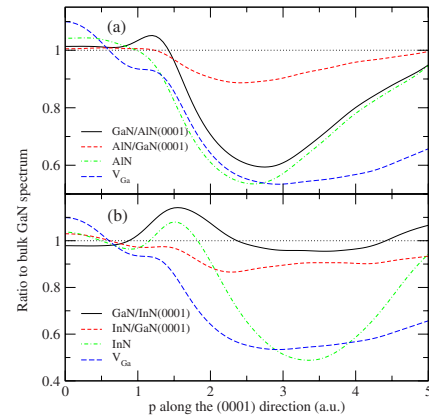


FIG. 4. (Color online) Doppler spectra calculated for the polar heterostructures (a) GaN/AlN(0001) and AlN/GaN(0001); (b) InN/GaN(0001) and GaN/InN(0001), shown as ratio to the bulk GaN spectrum. Also the corresponding ratios for bulk AlN and InN and the Ga vacancy in GaN are shown.

The positron energy offset defined above is similar to the concept of the positron affinity difference used to describe the positron's preference between two different metallic materials in contact.¹⁵ However, there are major differences. The positron affinities for metals can be considered as bulk properties, i.e., the difference for an interface does not depend on its structure. In semiconductor heterostructures, in contrast to the metallic systems, the charge transfer at the interfaces is governed by the availability of such physical electronic states at the interfaces that lie within the energy band gap.¹⁶ This makes the positron energy offset an interface-specific quantity. Moreover, in case of the polar heterostructures the formation of the macroscopic electric fields depends on the structure as a whole, as, in addition to the materials properties and strain, also the relative thicknesses of the layers play a role.^{17,18} When going toward larger layer thicknesses a simple electrostatic model¹⁸ predicts the magnitude of the electric fields to stay constant provided that the proportions of the heterostructure are held fixed. However, at larger thicknesses the corresponding potential drops across the nitride layers are limited by the energy band gaps of the respective materials.¹⁸

The most important question addressed in this Rapid Communication is whether positron annihilation spectroscopy could distinguish between a free positron state in a bulk semiconductor and a confined interface state in a polar heterostructure. We have calculated positron lifetimes and Doppler spectra for our heterostructure models. As mentioned above the predicted positron lifetimes do not show clearly measurable variations between the different systems and therefore their detailed discussion is omitted. In contrast, the Doppler spectra, which reflect the chemical environment sampled by the positron, are very sensitive to the increased positron overlap with the interface region. Figure 4 shows the Doppler spectra calculated for our four defect-free polar heterostructure models represented as a ratio to the bulk GaN spectrum. This representation highlights the changes due to the interface and strain with respect to the signal expected for unstrained, defect-free GaN. To facilitate comparison with a

signal from a sample with vacancy defects the corresponding ratio for the Ga vacancy in GaN (V_{Ga}) is also shown as well as the results for bulk AlN and InN for separating the effect of the interface on the spectra. The spectra show no anisotropy despite the confinement effect. We do not consider the nonpolar nitride heterostructure models in which positrons are not sensitive to the interface.

In the case of the systems containing both GaN and AlN [Fig. 4(a)], the maximum of the positron density is on the GaN side but there is significant overlap with AlN. Therefore, the resulting spectrum is approximately a linear combination of the GaN (constant ratio of 1) and AlN spectra. For the GaN/AlN(0001) system the lowering of the ratio curve at high momenta is of the same order of magnitude as that for the Ga vacancy in bulk GaN or for defect-free AlN. For the AlN/GaN(0001) system the overlap of the positron density with Ga d electrons is higher than in bulk Ga due to the smaller strained in-plane lattice parameters. This leads to higher intensity at high momenta. In the case of the GaN- and InN-containing systems [Fig. 4(b)], the peak below 2 a.u. in the GaN/InN(0001) spectrum is due to the InN contribution. The shape of the InN/GaN(0001) result resembles that of the Ga vacancy one. This is because the overlap with InN is small and the in-plane lattice parameters are larger than in bulk GaN, which leads to lower atomic density and reduced overlap with high-momentum core electrons. When analyzing the results of Fig. 4, one must, however, note that the shapes of the ratio spectra are sensitive to the resolution of the measurement, especially in regions where the raw spectra decrease fast, and a detailed quantitative analysis is not justified.

To confirm the effect of vacancies on the character of the positron state in the polar heterostructures we carry out calculations using laterally larger supercells with vacancy defects. We consider cation vacancies situated at different locations in the nitride layers and find that the positron always localizes at the vacancy irrespective of its location in the

system. The nitrogen vacancies do not trap positrons according to the calculations. The positron binding energy follows the behavior of the macroscopic electric field but the localized positron state at the vacancy is always energetically more attractive than the delocalized bulk state at the interface. Since there is a finite overlap between the confined interface state and the bulk parts of the layers, trapping at a vacancy is always possible. However, the positron trapping rate is expected to vary with the probability density of the initial positron state, i.e., with the distance from the attractive interface, roughly as the positron density in Figs. 2 and 3. According to our calculations, the positron annihilation characteristics reflect the immediate chemical environment of the vacancy without direct effects due to the macroscopic electric field.

In conclusion, we have performed first-principles modeling of positron states and annihilation in III-nitride heterostructures. The strain conditions and in the case of polar structures also the macroscopic electric fields affect the spatial confinement of the positron state. In nonpolar structures the positron density is spread across layers of the other material component. In polar heterostructures the positron samples the volume close to one of the two nonequivalent interfaces and the Doppler spectra are affected by both of the nitride materials resulting in a signal specific to the interface. If there are cation vacancies present in the polar heterostructures the macroscopic electric field does not prevent the positron from trapping at them although we expect the trapping rate to decrease with increasing distance of the vacancy from the preferred interface. Thus, positron annihilation measurements can be used to obtain information on the interface structures and vacancy-type defects in device structures based on III-nitrides or other wurtzite-structured systems such as the ZnO-related alloys.

The authors acknowledge funding from the Academy of Finland and the generous computer resources from CSC—IT Center for Science.

¹H. Morkoç, *Handbook of Nitride Semiconductors and Devices* (Wiley-VCH, Berlin, 2008), Vol. 1-3.

²M. A. Reshchikov and H. Morkoç, *J. Appl. Phys.* **97**, 061301 (2005).

³K. Saarinen, P. Hautojärvi, and C. Corbel, in *Identification of Defects in Semiconductors*, edited by M. Stavola (Academic Press, New York, 1998), Vol. 51A, p. 209.

⁴K. Saarinen *et al.*, *Phys. Rev. Lett.* **79**, 3030 (1997); K. Saarinen, in *III-Nitride Semiconductors: Electrical, Structural and Defects Properties* (Elsevier, Amsterdam, 2000), p. 109; S. Hautakangas, J. Oila, M. Alatalo, K. Saarinen, L. Liskay, D. Seghier, and H. P. Gislason, *Phys. Rev. Lett.* **90**, 137402 (2003); F. Tuomisto *et al.*, *Appl. Phys. Lett.* **86**, 031915 (2005); F. Tuomisto, V. Ranki, D. C. Look, and G. C. Farlow, *Phys. Rev. B* **76**, 165207 (2007).

⁵S. Hautakangas, I. Makkonen, V. Ranki, M. J. Puska, K. Saarinen, X. Xu, and D. C. Look, *Phys. Rev. B* **73**, 193301 (2006).

⁶F. Tuomisto, A. Pelli, K. M. Yu, W. Walukiewicz, and W. J. Schaff, *Phys. Rev. B* **75**, 193201 (2007).

⁷S. F. Chichibu *et al.*, *Nature Mater.* **5**, 810 (2006).

⁸F. Bernardini and V. Fiorentini, *Phys. Rev. B* **57**, R9427 (1998).

⁹F. Bernardini, V. Fiorentini, and D. Vanderbilt, *Phys. Rev. B* **56**, R10024 (1997).

¹⁰P. Lefebvre *et al.*, *Appl. Phys. Lett.* **78**, 1252 (2001).

¹¹P. E. Blöchl, *Phys. Rev. B* **50**, 17953 (1994).

¹²G. Kresse and J. Furthmüller, *Phys. Rev. B* **54**, 11169 (1996); G. Kresse and D. Joubert, *ibid.* **59**, 1758 (1999).

¹³I. Makkonen, M. Hakala, and M. J. Puska, *Phys. Rev. B* **73**, 035103 (2006).

¹⁴A. Baldereschi, S. Baroni, and R. Resta, *Phys. Rev. Lett.* **61**, 734 (1988).

¹⁵M. J. Puska, P. Lanke, and R. M. Nieminen, *J. Phys.: Condens. Matter* **1**, 6081 (1989).

¹⁶C. G. Van de Walle, J. L. Lyons, and A. Janotti, *Phys. Status Solidi A* **207**, 1024 (2010).

¹⁷X. Y. Cui, D. J. Carter, M. Fuchs, B. Delley, S. H. Wei, A. J. Freeman, and C. Stampfl, *Phys. Rev. B* **81**, 155301 (2010).

¹⁸V. Fiorentini, F. Bernardini, F. Della Sala, A. Di Carlo, and P. Lugli, *Phys. Rev. B* **60**, 8849 (1999).